Research of the Unmanned Vehicle Control and Modeling for Lane Tracking and Obstacle Avoidance

Sang-Gyum Kim*, Woon-Sung Lee**, and Jung-Ha Kim***

* Graduate School of Automotive Engineering, Kookmin University, Seoul, Korea
(Tel : +82-2-916-0991; E-mail:ssanggyum @hanmail.net)
** Graduate School of Automotive Engineering, Kookmin University, Seoul, Korea
(Tel : +82-2-910-4712; E-mail: wslee@kookmin.ac.kr)
*** Graduate School of Automotive Engineering, Kookmin University, Seoul, Korea
(Tel : +82-2-910-4715; E-mail: jhkim@kookmin.ac.kr)

Abstract: In this paper, we will explain about the unmanned vehicle control and modeling for combined obstacle avoidance and lane tracking. First, obstacle avoidance is considered as one of the important technologies in the unmanned vehicle. It is consisted by two parts: the first part includes the longitudinal control system for the acceleration and deceleration and the second part is the lateral control system for the steering control. Each system uses to the obstacle avoidance during the vehicle moving. Therefore, we propose the method of vehicle control, modeling and obstacle avoidance. Second, we describe a method of lane tracking by means of vision system. It is important in the unmanned vehicle and mobile robot system. In this paper, we deal with lane tracking and image processing method and it is including lane detection method, image processing algorithm and filtering method.

Keywords: Unmanned Vehicle, Ultrasonic Sensor, Obstacle Avoidance, Laser Scanner, Lane Tracking, CCD Camera.

1. INTRODUCTION

During the past decade considerable effort has been made to develop an unmanned vehicle for a variety of applications in the military, surveillance, terrain mapping and emergency environment, and vehicle safety, and this effort has recently been associated with social infrastructure. Also, most unmanned vehicles use variable sensors for vehicle safety and accurate vehicle control. Therefore, research into hardware and software control is very important for vehicle operation. Recently, research of most vehicles has been focused on the vehicle stability and customer satisfaction, including riding convenience, reduced emission, and fuel-efficient advantage.

In this paper, we will explain about the unmanned vehicle control and modeling for combined obstacle avoidance and lane tracking. First, obstacle avoidance is considered as one of the important technologies in the unmanned vehicle. It is consisted by two parts: one longitudinal control system for the acceleration and deceleration and a lateral control system for the steering control. Each system uses to the obstacle avoidance during the vehicle moving. Therefore, we propose the method of vehicle control, modeling and obstacle avoidance. Second, we describe a method of lane tracking by means of vision system. It also is important in the unmanned vehicle and mobile robot system. Therefore, we deal with lane tracking and image processing method and it is including lane detection method, image processing algorithm and filtering method.

Finally, in this research, those present above resultant though simulation, vehicle test, vision system and data communication.

2. VEHICLE CONTROL SYSTEM OF UNMANNED VEHICLE

2.1 Longitudinal control

In the research, the longitudinal control of a vehicle is operated by a DC motor control and brake control. Generally, DC motor is a number of merit; small rotor size, high power density, low inertia, fast dynamic response, high speed/torque capability, low maintenance cost, high torque/inertia ratio and better heat dissipation. The most eminent merit of the Brush-less DC motor is the removal of the brushes. These can be used in dangerous environments or even then under-water vehicle applications.

The motor driving system is controlled by the input voltage to the motor by digital signal processing and conversion to an analog signal by a D/A converter.

The vehicle's velocity is calculated from the wheel rotation, which is measured by counting a Hall sensor signal per unit time. The velocity data use total vehicle moving distance calculation, which also is used as a velocity profile for path planning. The traction motor controller is used for the vehicle driving control through a traction motor. It is controlled by a voltage signal to the motor rotation so it generates the driving torque, which causes wheel rotation. Consequently, the vehicle velocity and distance are calculated from the wheel rotation counter.

2.1.1 Driving system modeling

In this paper, we used the DC motor modeling for vehicle control of longitudinal distance. It directly provided rotary motion and, coupled with wheels or drums and cables, provided transition motion. The electric circuit of the armature and the free body diagram of the rotor are shown in Fig. 1. The control objective was determined by vehicle velocity and safe distance maintenance [1].

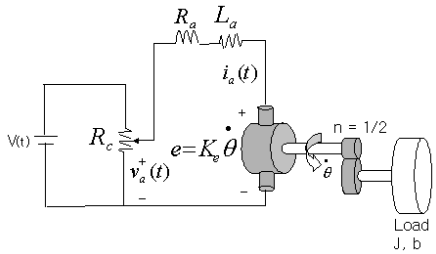

Fig. 1 Wire Model of Traction System

The armature voltage of the motor-electro approval, v_a (t) is controlled proportionally to the source voltage $V(t)$ of the equal circuit, where i_a (t) is the armature current, R_a is the electric resistance, L_a is the electric inductance component of the electric windings, and e is a counter-electromotive force

conduction of electricity while the motor is rotating. From the figure above we can write the following equations based on Newton's law combined with Kirchhoff's law. The torque, T can be written, as in Eq. 1, where J is the moment inertia of the motor, b is damping ratio of the mechanical system, and k_t is the armature constant.

$$T = k_t i_a = J\frac{d\dot{\theta}}{dt} + b\dot{\theta} \tag{1}$$

Generally, electric voltage is conducted proportionally by the magnetic velocity and angular velocity as the magnetic field rotates. Therefore, e is related to the rotational velocity by the following equations.

$$e = k_e\dot{\theta} \tag{2}$$

where, k_e is the counter-electromotive force constant. The voltage equation of the equivalent circuit is related by the following equations.

$$V(t) = k_a v_a(t) \tag{3}$$

$$v_a(t) - e = R_a i_a + L_a\frac{di_a}{dt} \tag{4}$$

where, electric resistance R_a and counter electromotive force k_e are constant, and it is assumed that all initial conditions are zero. Using Laplace Transforms of the above modeling equations, we get the following transfer function, where the rotating speed is the output and the voltage is an input.

$$\frac{\dot{\theta}(s)}{V(s)} = \frac{k_a k_t}{(R_a + L_a s) + (Js + b) + k_t k_e} \tag{5}$$

Fig. 2 shows the system closed-loop block diagram of transfer function of Eq. 5.

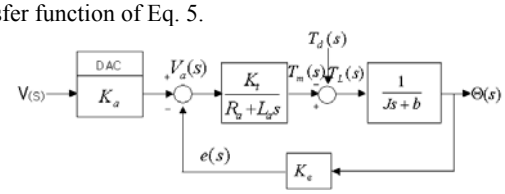

Fig. 2 Close-loop block diagram of traction system

Exact values for the motor rotor inertia, electric resistance, and electric inductance values are difficult to determine. Therefore, this research has determined the transfer function through iterative experiments as an approximate value. Fig. 3 shows the motor velocity profile for a step input voltage and the simulation result of the transfer function, which is expressed in the MATLAB program m-file to verify the transfer function. This experiment was performed using the *Lab-View* software.

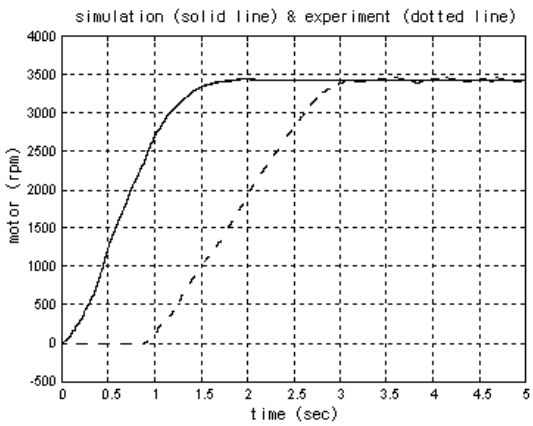

Fig. 3 Comparison of DC motor transfer function between experiment and simulation results

We have found the natural frequency and damping ratio, which are used to get the transfer function. The traction function of the traction system can be rewritten as Eq. 6.

$$G(s) = \frac{\Theta(s)}{V(s)} = \frac{5866.575}{s^2 + 4.55s + 7.111} \tag{6}$$

2.2 Lateral control

The steering actuator for accuracy steering control uses a stepping motor, which uses a timing belt to connect with the steering column.

The steering torque of steering column is estimated by a torque measurer, which required about 20[Kg·cm]. Therefore, in this experiment we chose a stepping motor (PK-296 model) to overcome the force of reaction that has a 1400 [g·cm^2] rotor inertia moment and a maximum holding torque of 22 [Kg·cm]. This stepping motor torque is controlled by a 10:1 reduced gear ratio.

The experiment's results show that total steering angleis 1080 degrees and the total number of pulse is 12,000. So, factor (α) of the relationship input pulse and the steering angle is defined as

$$\alpha = \frac{360^\circ}{4000}[\deg/pulse] = 0.09[\deg/pulse]$$
$$\frac{1}{4000}[rev/pulse] = 0.00025[rev/pulse] \tag{7}$$

Eq. 7, we know the maximum resolution is about 0.18 degree.

2.2.1 Steering system modeling

The bicycle model is used for a precise and improved steering system of an unmanned vehicle [2-3]. We considered that the vehicle has to disregard rolling the motion on normal road conditions and driving constant velocity. If the vehicle, moving on a normal road, has acceleration on the lateral side, the acceleration occurs about the normal direction and the vehicle has acceleration. This is considered the cornering force. Fig. 4 shows the dynamic motion parameters of the steering system, which is expressed as the coordinate system for the bicycle model.

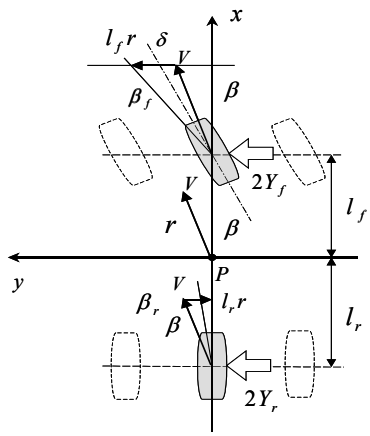

Fig. 4 Bicycle model for steering system modeling

δ means that the steering angle is all the front wheels about the vehicle of front and real direction, the front and rear bilateral wheel sideslip angles of each tire is β_{f1}, β_{f2}, β_{r1}, β_{r2}, and the cornering forces of tire are Y_{f1}, Y_{f2}, Y_{r1}, Y_{r2}.

The cornering force of the front and rear wheels is assumed to be K_f and K_r. The sideslip angle is positive and applied in a negative direction from the Y axis.

From the figure above we can write the following equations about bicycle modeling.

$$mV\frac{d\beta}{dt}+2(K_f+K_r)\beta+\{mV+\frac{2}{V}(l_fK_f-l_rK_r)\}r=2K_f\delta \quad (8)$$

$$2(l_fK_f-l_rK_r)\beta+I\frac{dr}{dt}+\frac{2(l_f^2K_f+l_r^2K_r)}{V}r=2l_fK_f\delta \quad (9)$$

We can lead to motion equation from yawing angle velocity of the input steering angle through of the Eqs. 8 ~ 9. It is able to Laplace transformation yields

$$\frac{R(s)}{\Delta(s)}=\frac{2(mVl_fK_fs+(l_fK_f^2+2K_fK_r(2l_f-l_r))}{mVI(s^2+\frac{2m(l_f^2K_f+l_r^2K_r)+2I(K_f+K_r)s}{mIV}+\frac{4K_fK_rV^2}{mIV^2}-\frac{2(l_fK_f-l_rK_r)}{I})} \quad (10)$$

Also, it is impossible for accurate measurement that is transfer function of the system parameter K_f, K_r, and the vehicle yawing the moment of inertia *I*. Therefore, in this research, these parameters were determined experimentally. We obtained the steering angle (δ) using a gyro sensor.

Fig. 5 shows the measured response of the vehicle to a step input and simulation result to the steering angle (δ). The system transfer function of Eq. 11 leads to many experiments in Fig. 5.

$$G(s)=\frac{R(s)}{\Delta(s)}=\frac{97.3}{s^2+2.31s+2.78} \quad (11)$$

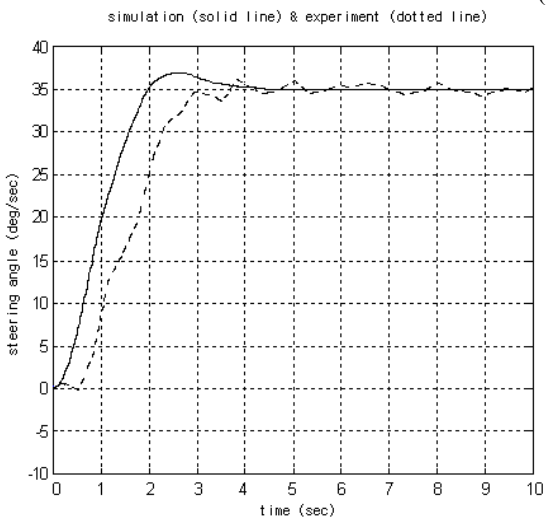

Fig. 5 Comparison of steering angle transfer function between experiment and simulation results

The result of the modeling response agrees with the experimentally measured values. However, the result does not show accurate agreement with the experimental results due to the noise and incomplete tuning. But the settling time, rasing time and steady-state error are almost similar. More accurate experiment conditions and tuning would make it possible to determine exactly the transfer function for the steering control.

3. SENSOR SYSTEM OF UNMANNED VEHICLE

3.1 Ultrasonic sensor and laser scanner

In the research, ultrasonic sensors and laser scanner are used for obstacles detecting and obstacle avoidance when the vehicle is in motion. Generally, the distance measurement signal of the ultrasonic sensor and laser scanner is converted into digital data by an A/D converter, and it calculates distance to the main computer according to a pic-process and DAQ board signal. The distance among the ultrasonic sensor, laser scanner and the obstacle is measured by the ultrasonic sensor and laser scanner principle. Fig. 8 shows the principle of the time variable gain amplifier and the functional diagram of the ultrasonic sensor. Fig. 9 shows the scanning field of the laser scanner. Generally, the laser scanner works by measuring the time of flight of laser light pulses. The pulsed laser beam is deflected by an internal rotating mirror so that a fan-shaped scan is made of the surrounding area. The shape of the object is determined by the sequence of impulses received. The scanner's measurement data can be individually processed in real time with external evaluation software. Standard solutions are also available for object measurement. The unit communicates with the host computer using an RS232 serial interface card.

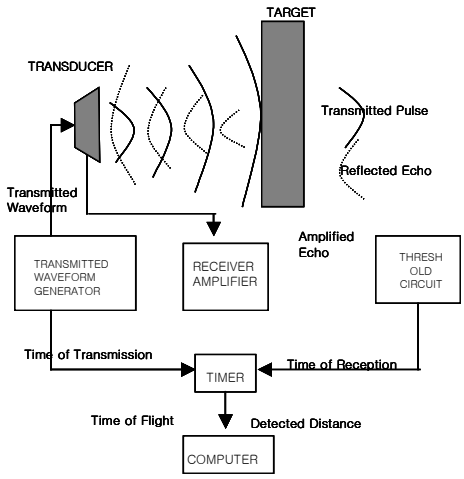

Fig. 8 Functional diagram of ultrasonic sensor

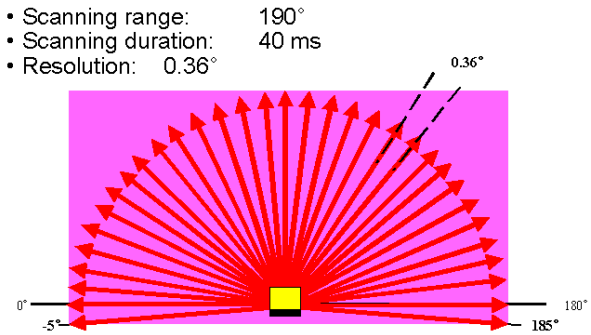

Fig. 9 Scanning field of the laser scanner

The position attached on the vehicle of ultrasonic sensors and laser scanner shown in Fig. 10.

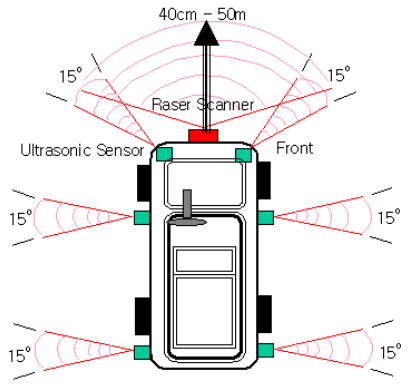

Fig. 10 Position of ultrasonic sensors & laser scanner

3.2 Vision system

The vision of an unmanned field can be considered from the application of computer vision techniques to industrial

automation. Unmanned vehicle vision has now been an active area of research for several decades, and it is gradually being introduced for the real-world application. A typical vision system processing method, shown in Fig. 11 and it consists of a camera, a vision interface processor, or "frame-grabber," and a computer system to process and interpret data [4].

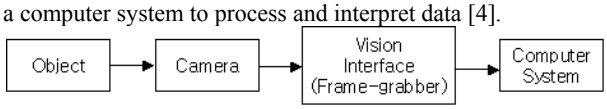

Fig. 11 Vision system components

3.2.1 Road model

Generally, the road information is obtained through a camera, but it is not correct to use for control because a camera has a two-dimensional coordinate system and vehicle control needs a three-dimensional coordinate system. Therefore, it needs conversion processing to a three-dimensional from a two-dimensional coordinate system, which is called inverse perspective mapping. Also, to obtain a road image from two coordinate systems, we should have decided at the lens parameter, the height of the camera on the vehicle, and a few different parameters. In this research, we used the real coordinate system, which is known through the road model. So we must convert the image coordinate into the real coordinate. Fig. 12 shows the *X, Y* plane and $Z\eta$ plane of the real coordinate system according to camera location and real coordinate system, which is changed by means of camera location.

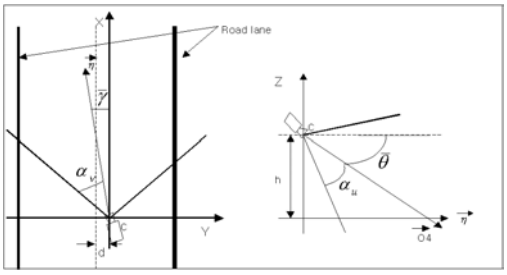

Fig. 12 Relationship between Image Coordinate and Real Coordinate

The coordination conversion equation is written as the real coordinate system as follows:

$$u(x,y,0)=\frac{\tan^{-1}\left[\dfrac{h\cdot\sin\{\tan^{-1}(\frac{y}{x})\}}{y}\right]-(\bar{\theta}-\alpha_u)}{\dfrac{2\alpha_u}{n-1}} \tag{12}$$

$$v(x,y,0)=\frac{\tan^{-1}(\frac{y}{x})-(\bar{r}-\alpha_v)}{\dfrac{2\alpha_v}{m-1}} \tag{13}$$

The conversion of the image coordinate into the real coordinate is expressed as the following equations:

$$x(u,v)=\frac{h}{\tan\{\bar{\theta}+(\frac{2u}{n-1}-1)\alpha_2\}}\cdot\cos\{\bar{r}+(\frac{2v}{m-1}-1)\alpha_1\} \tag{14}$$

$$y(u,v)=\frac{h}{\tan\{\bar{\theta}+(\frac{2u}{n-1}-1)\alpha_2\}}\cdot\sin\{\bar{r}+(\frac{2v}{m-1}-1)\alpha_1\} \tag{15}$$

3.2.2 Image process for lane detection

Thresholding is one of the most generally using methods in an image process method and is expressed as a black and white (grayscale) value of a digital image. In this research, it is expressed as a lightness value of 0 or 255. This image grayscale has a bright resolution of 8 bits and is expressed as 320*240 pixels.

The critical value must be determined for thresholding, and it set at a standard value for divided at a character of image to drawing out particular information, and the critical value must be determined for drawing out the lane from the road image. In this research, critical values have been determined many times through experiment. Fig. 13 shows at image of a road according to a change of critical values.

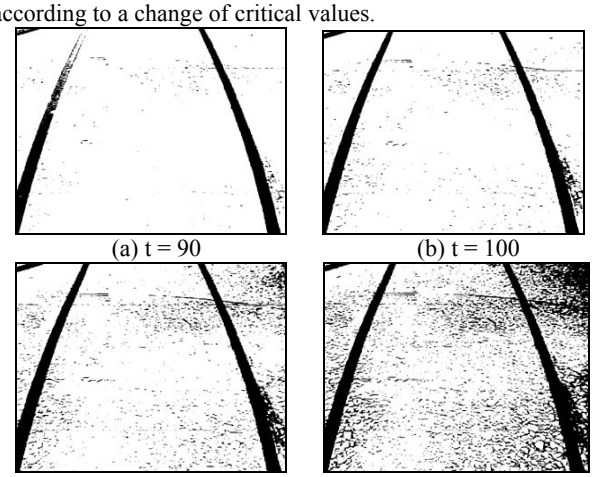

(a) t = 90 (b) t = 100

(c) t = 110 (d) t = 120

Fig. 13 Image of different threshold value (t)

Fig. 13, (a) shows a thresholding image in the case of critical value = 90, which we know removes noise and some of the lane at the same time. Fig. 13, (c) shows the case of critical value =110, which we know clears the lane but includes noise. Fig. 13, (b) shows a thresholding image in the case of critical value = 100, which we know clears noise and compares with another image, and the noise is removed through filtering.

3.2.3 Filtering

Generally, filtering is defined as removing the noise. Therefore, in this research, we removed noise using a median filtering method. Fig. 14 shows as a process method of median filtering and in the figure the pixel value within the solid line and dotted line mean as average value of 4, also it is shown changed 10 and 3 values and noise can be removing through this process.

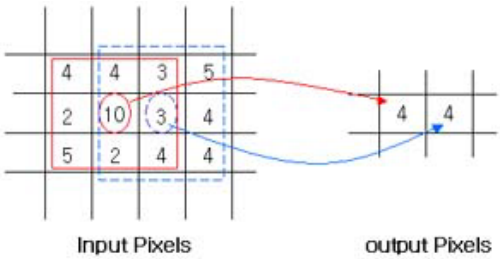

Fig. 14 Method of median filtering

4. TEST EVALUATION

4.1 Ultrasonic sensor

Obstacle detection and avoidance experiment estimation are one of the foremost experiments in unmanned vehicles. The ultrasonic sensor is one of the range sensors, which can

measure a distance to objects, and it is more commonly used with unmanned vehicle and mobile robots because it is small, inexpensive and it is easy to calculate the object's distance.

The first experiment stage is environment detecting by the corridor and finding the center position of bilateral wall with ultrasonic sensor. Fig. 15 shows the test result of ultrasonic sensors character experiment, and it shows average distance values from the centerline of the corridor to the wall and the sensor error rate from the centerline to the wall.

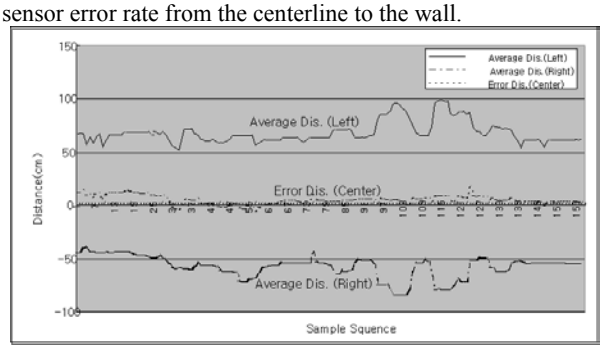

Fig. 15 Ultrasonic sensor experimental result in corridor [average and error rate]

Fig. 16 compares the test results of the ultrasonic sensors and it condition experimental adhere to front side two sensors and real side two sensors and each sensors signal measure a distance of between the vehicle and corridor wall, and each curve shows a state of the corridor wall. We know from the results that it is only a small-time delay and it shows a similar trend from the sensor signal.

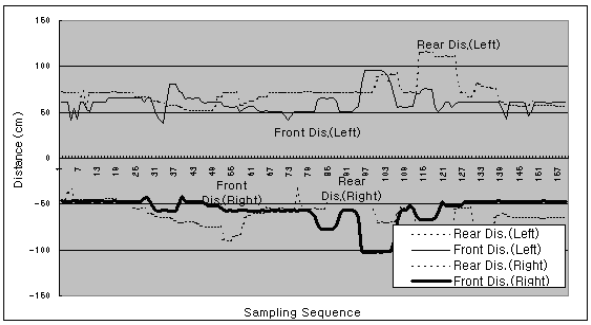

Fig. 16 Ultrasonic sensor experimental result in corridor [compare of sensor signal]

As the result of another experiment, Fig. 17 compares the test results of S-turn driving under the same conditions. We know from the results that it is only small-time delay and it shows a similar trend from the sensor signal.

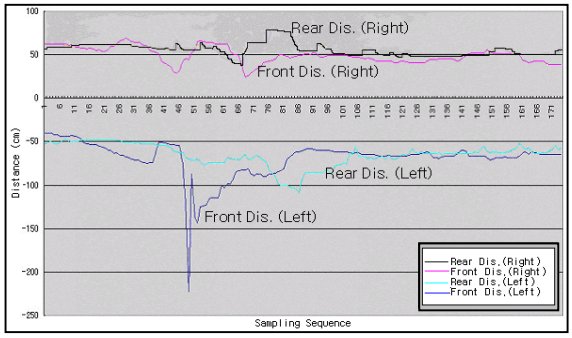

Fig. 17 Ultrasonic sensor experimental result in corridor [compare of sensor s-turn signal]

The second experiment concerns the object avoidance method of an ultrasonic sensor. Fig. 18 shows the test environment on the road, which has an obstacle in the front.

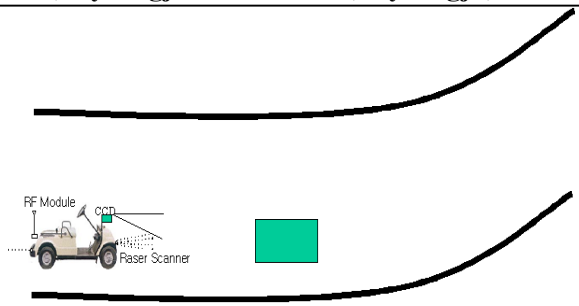

Fig. 18 Environment of road, which has an obstacle in the front

Figs. 19 ~ 20 show the display software to detect an obstacle and the result of the path planning. We made a display board using a visual basic program to see all the necessary information about the object, such as size, data, and environment (road) profile.

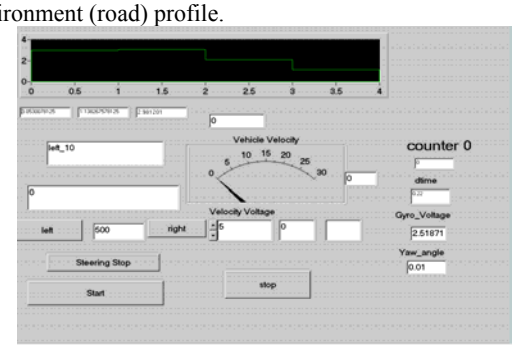

Fig. 19 Display of detecting obstacle [visual basic]

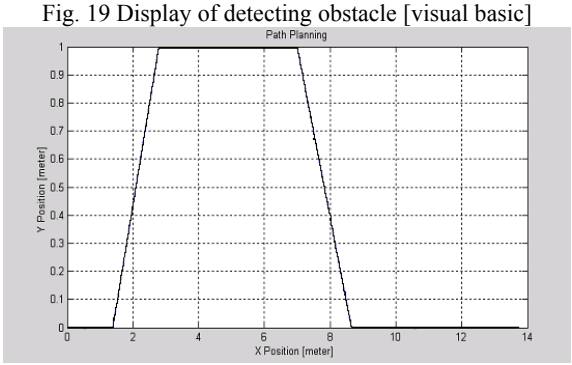

Fig. 20 The Experimental Result of the Path Planning

Fig. 21 shows the collision avoidance trajectory for an unmanned vehicle in the Fig. 18 condition, which used an ultrasonic sensor and laser scanner algorithm for reducing the calculation time and error rate. The vehicle trajectory of collision avoidance is larger than the minimum radius of the target trajectory because the ultrasonic sensors and laser scanner are giving an unstable signal output on the vehicle experiment. This problem can be solved by using ultrasonic sensor signal filtering and developing the more advanced control algorithm, such as PID control and fuzzy logic.

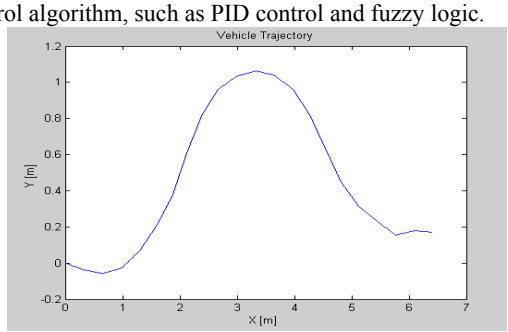

Fig. 21 Vehicle trajectory of collision avoidance

4.2 Driving experimental result of lane detection

The data were obtained through the vision board, which is used for vehicle control. The experiment consists of driving along the lane on road. And, it can be classified into two types experiments. The first experiment is lane detection using a CCD camera. The second experiment is vehicle control using a vision system and communication. We compared the difference between wire communication and wireless communication. Fig. 22 shows a lane position plot of road through wire communication between the vehicle system and the control main computer.

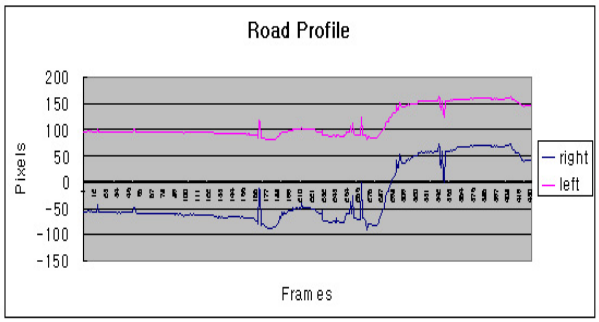

Fig. 22 Lane data profile using wire communication

Fig. 23 shows the road profile using a wireless RF module with added noise. Also, the wireless module has many errors because is uses high frequency.

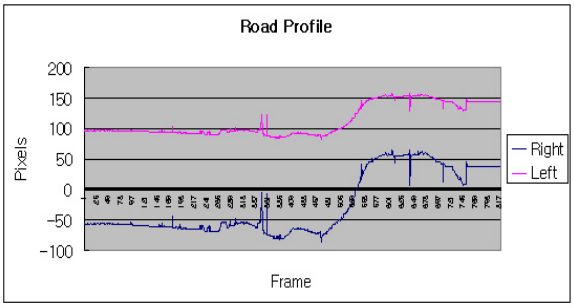

Fig. 23 Lane data profile using at a wireless RF module

Through the previous experiment, we know that the wire communication experiment is clearer in the lane detection compared with the wireless communication. Also, most wireless modules include a constant noise because of not remove at a noise during the image transmission.

4.3 Steering experimental result of lane detection

Figs. 24 ~ 25 show a steering angle according to the vehicle test. The experiment compares wire and wireless conditions.

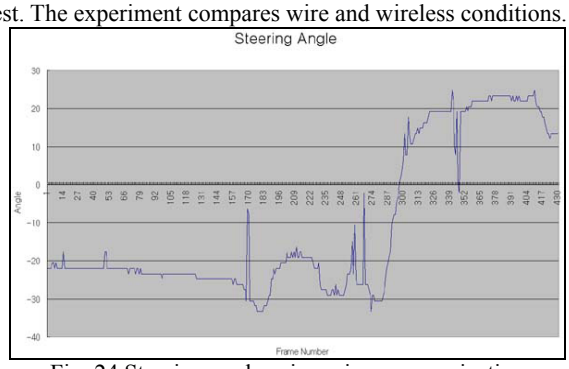

Fig. 24 Steering angle using wire communication

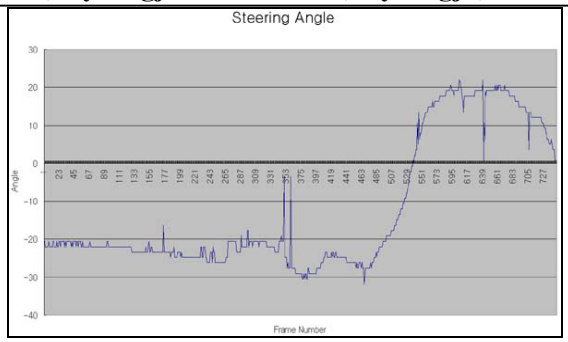

Fig. 25 Steering angle using wireless communication

From the experiment, we know that wire communication maintains a steering angle compared to wireless communication. The problem with wireless environments is that it brings on data lose according to transmission of the steering value, which brings on incorrect of the lane detection.

5. CONCLUSION

In this research, we showed the vehicle modeling and design analysis of an unmanned vehicle system for a lane tracking and an obstacle avoidance. For a longitudinal control, we used of the DC motor. In lateral control, the vehicle is controlled by a gyroscope, an ultrasonic sensor, vision sensor, and PID control was designed for reducing a steady-state error, rising time. And we explain the image processing method for lane detection by using a vision system. The performance of the system was evaluated through a vehicle test.

For more precise control, analysis and signal process require a variable experiment method and algorithm development, which will be used for advanced lateral control. This research on obstacle avoidance and lane tracking can be used in places where humans cannot go. This could have a military application: a robot could go in a minefield where it would be very dangerous for humans.

ACKNOWLEDGEMENT–The paper was support by the Brain Korean 21 project.

REFERENCES

[1] M. S. Kim, The System Modeling for Unmanned Vehicle & Autonomous Driving Technique by Ultrasonic Sensors, *Master's Thesis*, Graduate School of Automotive Engineering, Kookmin University, Seoul, Korea, 2001.

[2] C. R. Dorf and H. R. Bishop, *Modern Control Systems*, Addison Wesly, 1997.

[3] D. G. Thomas, *Fundamentals of Vehicle Dynamics*, Society of Automotive Engineering (SAE), 1992.

[4] A. J. Critchlow, *Introduction to Robotics*, Macmillan Publishing Co., New York, 1985.